

**Electronic Supplementary Information**

**A microwave-powered continuous fluidic system for polymer nanocomposite  
manufacturing: A Proof-of-Concept Study**

Milad Torabfam<sup>1</sup>, Mona Nejatpour<sup>1</sup>, Tuce Fidan<sup>1</sup>, Hasan Kurt<sup>2,3,4</sup>, Meral Yüce<sup>1,5</sup> and Mustafa  
Kemal Bayazit<sup>1,\*</sup>

<sup>1</sup>Faculty of Engineering and Natural Science, Sabanci University, 34956 Istanbul, Turkey

<sup>2</sup>Istanbul Medipol University, School of Engineering and Natural Sciences, Istanbul, 34810,  
Turkey

<sup>3</sup>Research Institute for Health Sciences and Technologies (SABITA), Istanbul Medipol  
University, Istanbul, 34810, Turkey

<sup>4</sup>Nanosolar Plasmonics, Ltd., Kocaeli, 41400, Turkey

<sup>5</sup>Sabanci University Nanotechnology Research and Application Center, Tuzla, Istanbul 34956,  
Turkey

E-mail:[mkbayazit@sabanciuniv.edu](mailto:mkbayazit@sabanciuniv.edu)

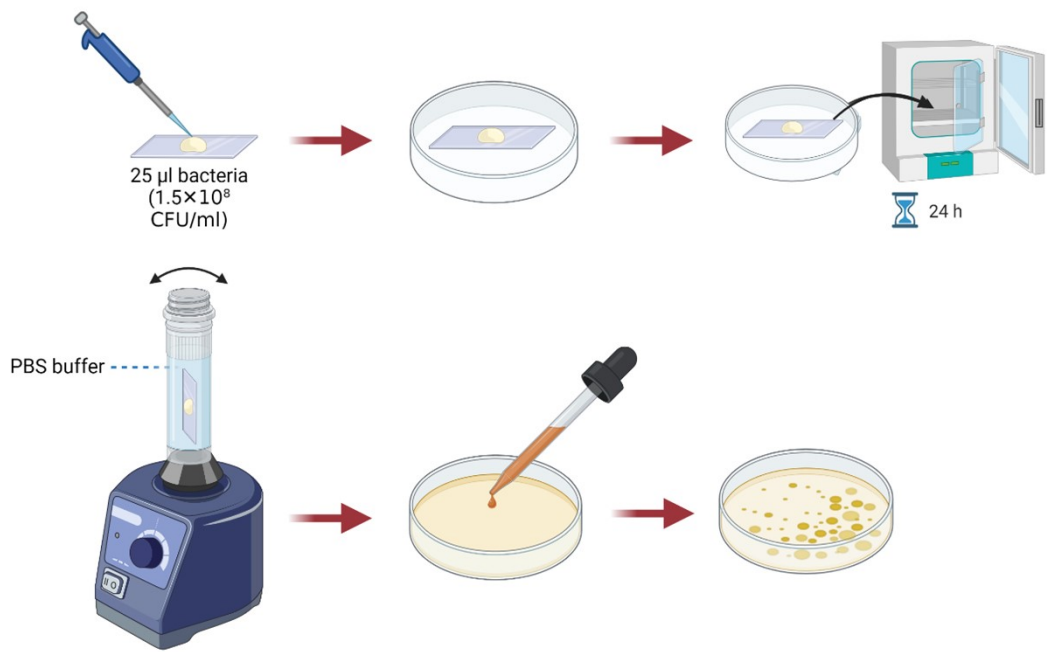


**Figure S1.** Graphical illustration of method applied on PA6 and NC coated glasses for evaluation of their antibacterial efficiency

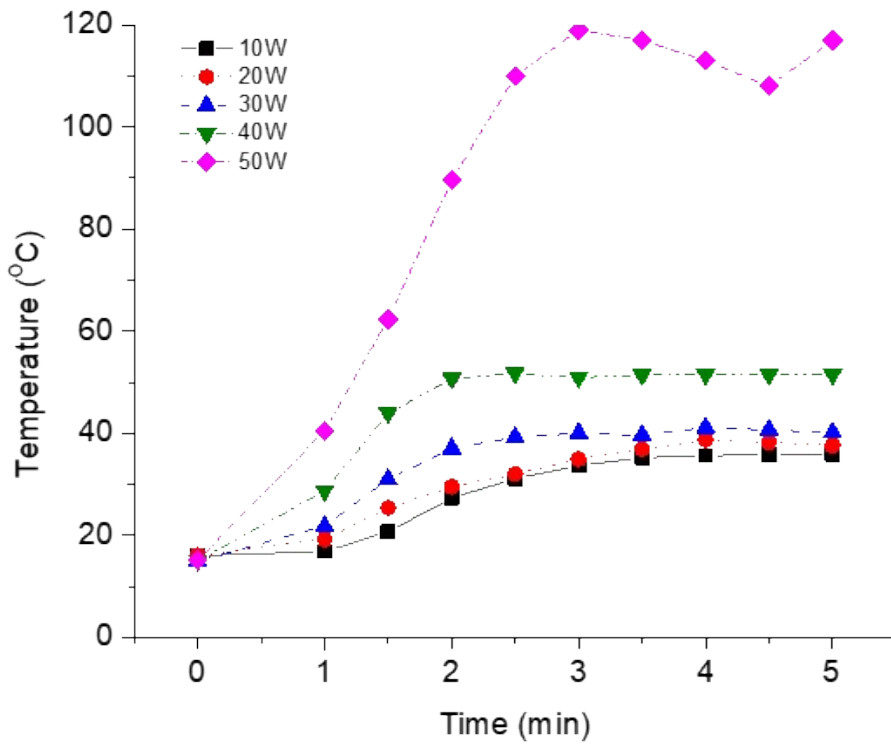


**Figure S2** The microwave power-dependent heating profile of the reaction fluid (PA6, AgNO<sub>3</sub>, and NaBH<sub>4</sub> solution in FA) in the MWFS under 20 psi constant pressure at the microwave powers of 10, 20, 30, 40, and 50 W. The temperature of the mixture was measured for 5 minutes at time intervals of 30 seconds.

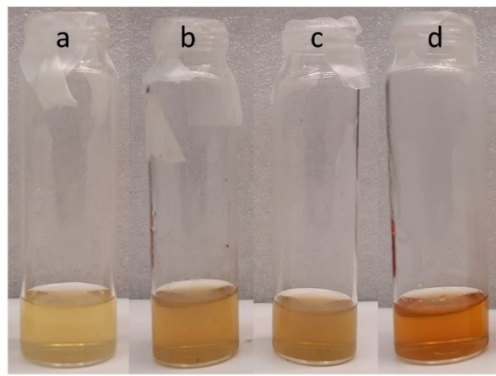


**Figure S3** Color of the prepared AgNP/PA6 NCs<sub>MWFs</sub> using MWPs of a) 10W, b) 20W, c) 30W, and d) 40W.

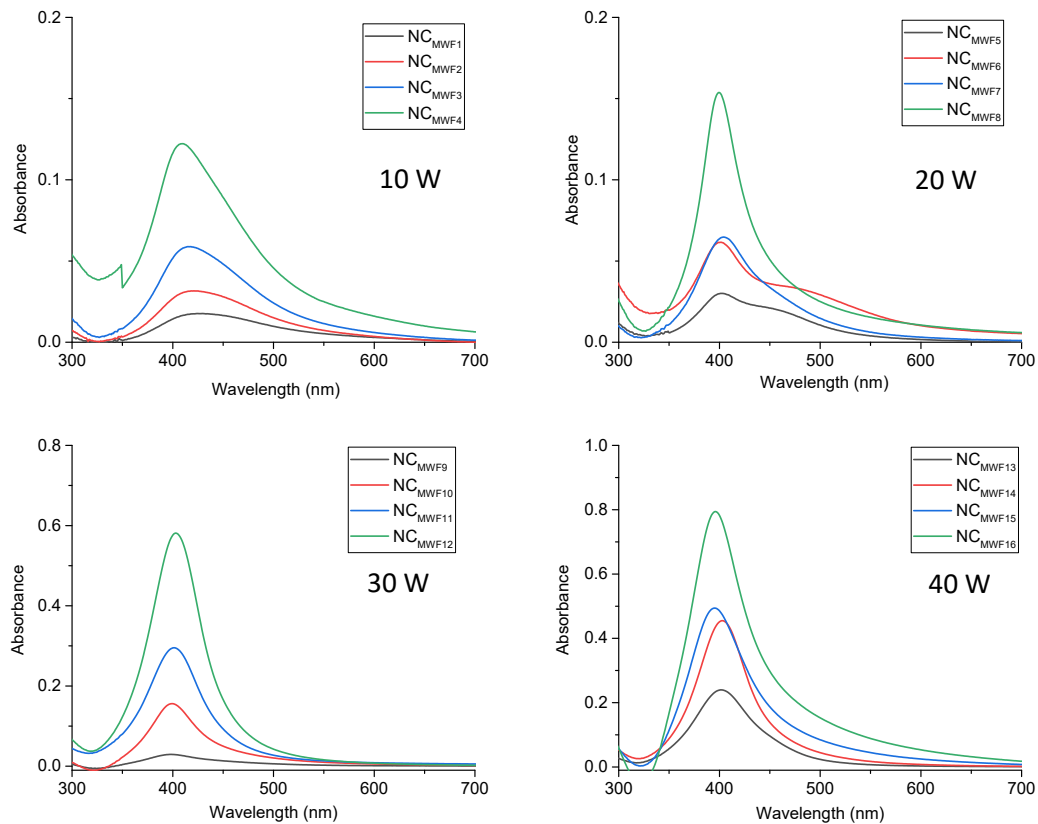


**Figure S4** UV-vis spectra of NC<sub>MWF1-16</sub>.

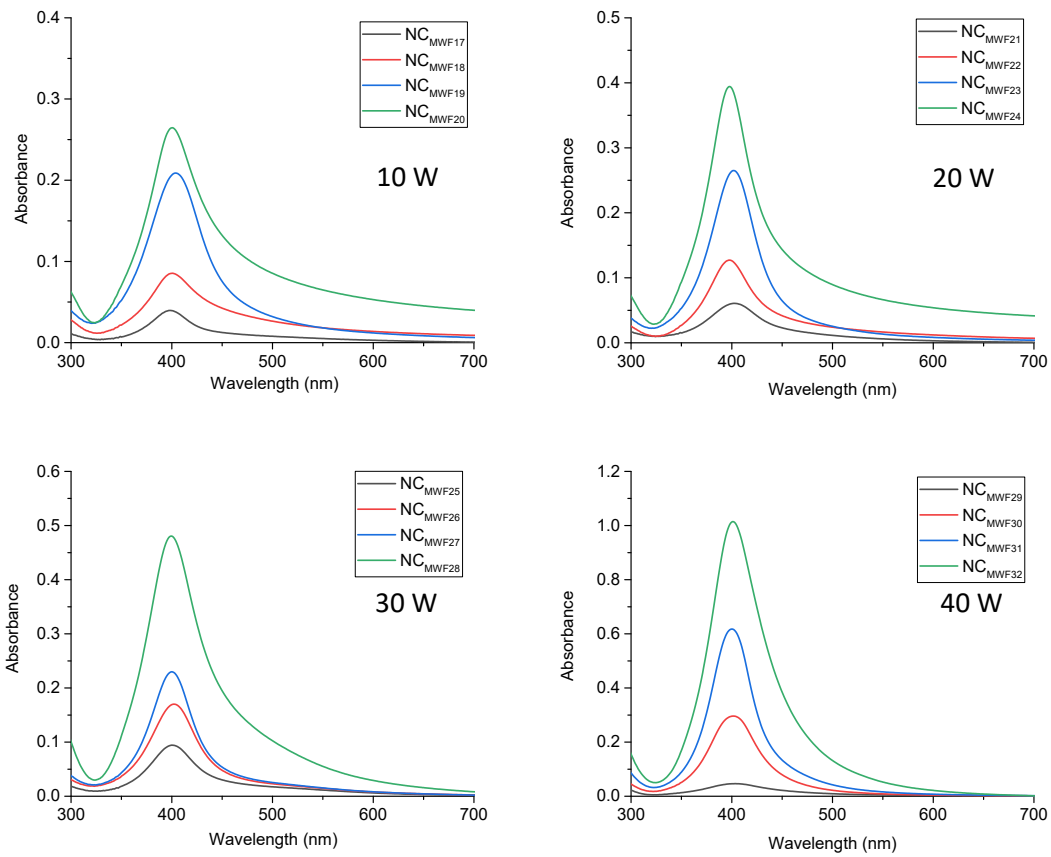


**Figure S5** UV-vis spectra of NC<sub>MWF17-32</sub>.

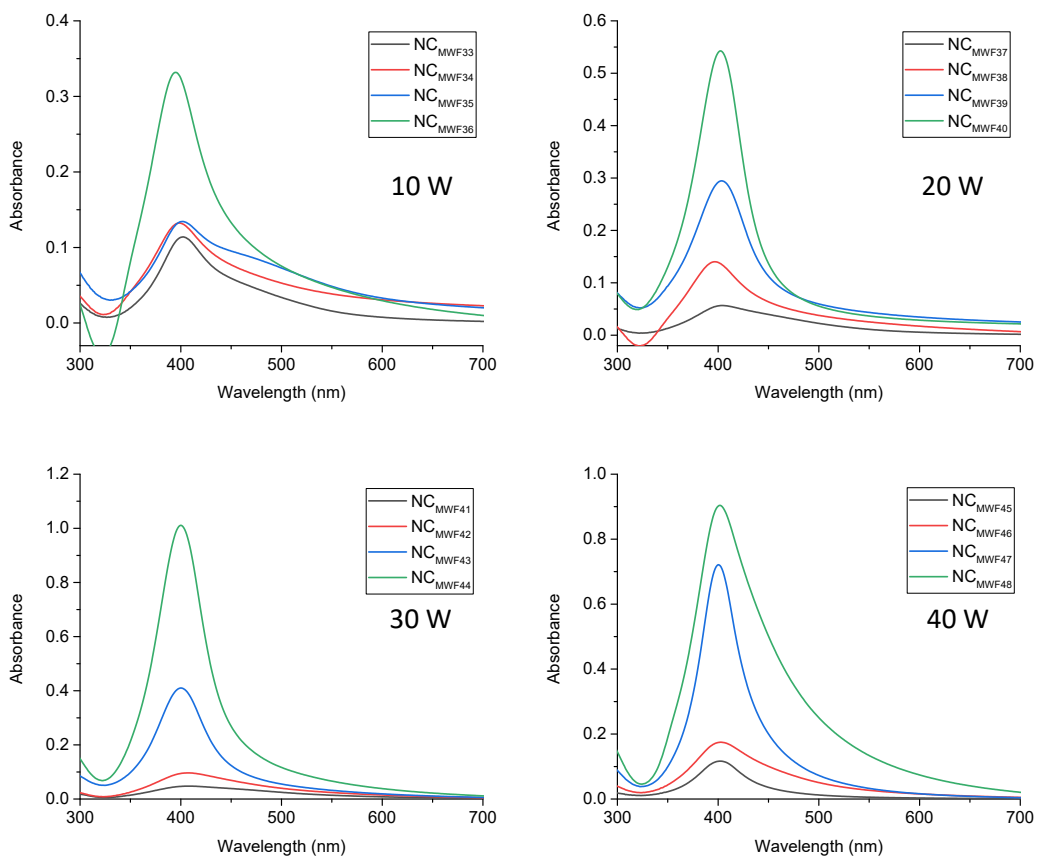


**Figure S6** UV-vis spectra of NC<sub>MWF33-48</sub>.

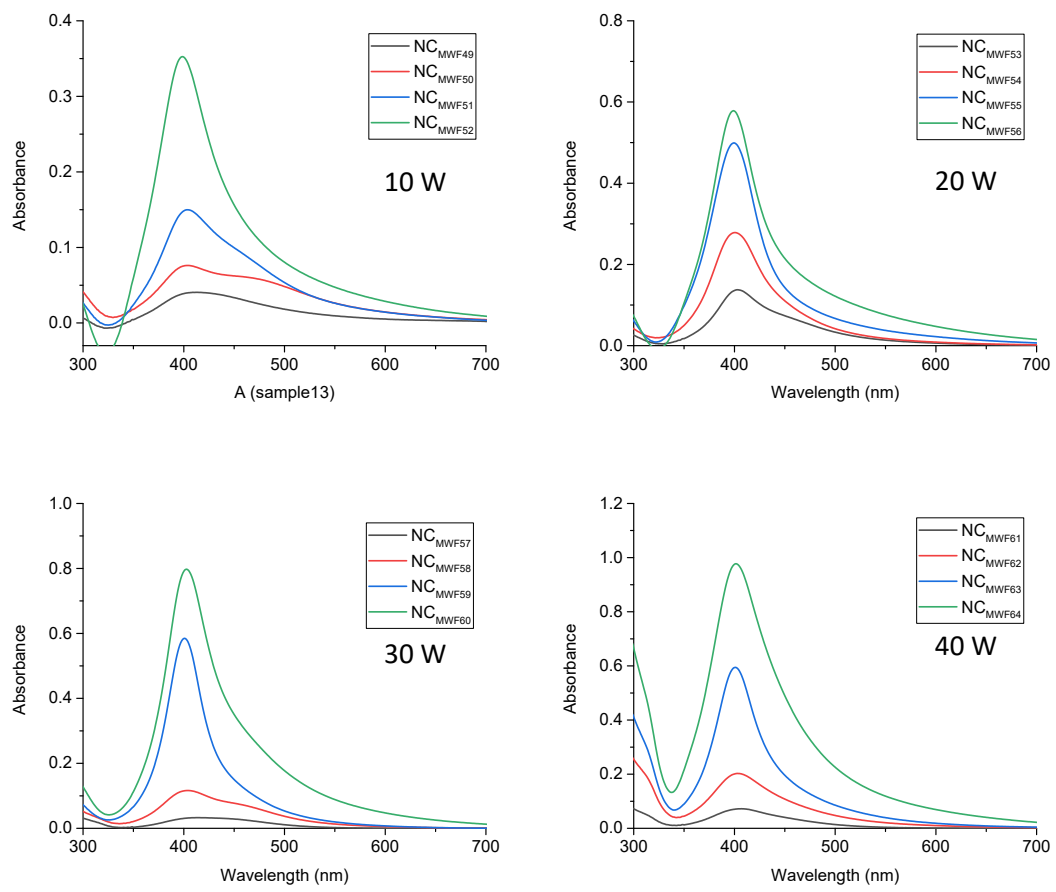


**Figure S7** UV-vis spectra of NC<sub>MWF49-64</sub>.

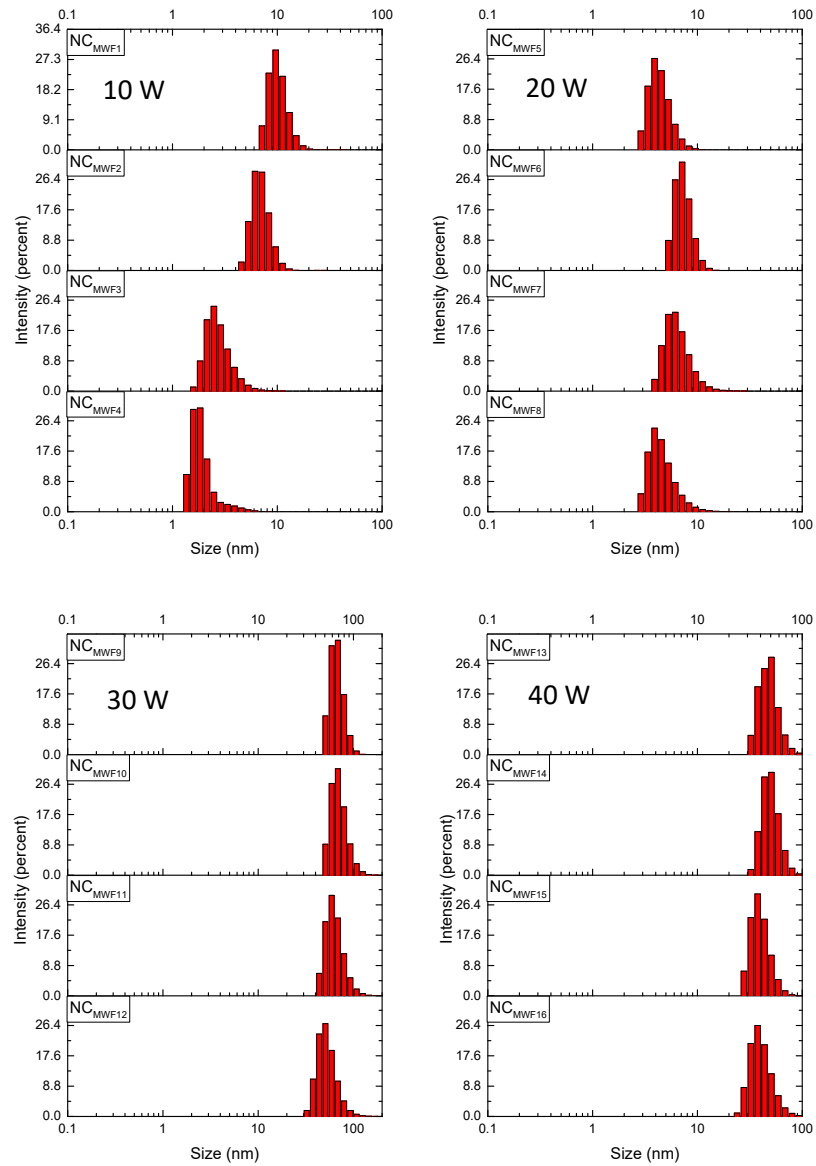


**Figure S8** Hydrodynamic size distribution of NC<sub>MWF1</sub>-16.

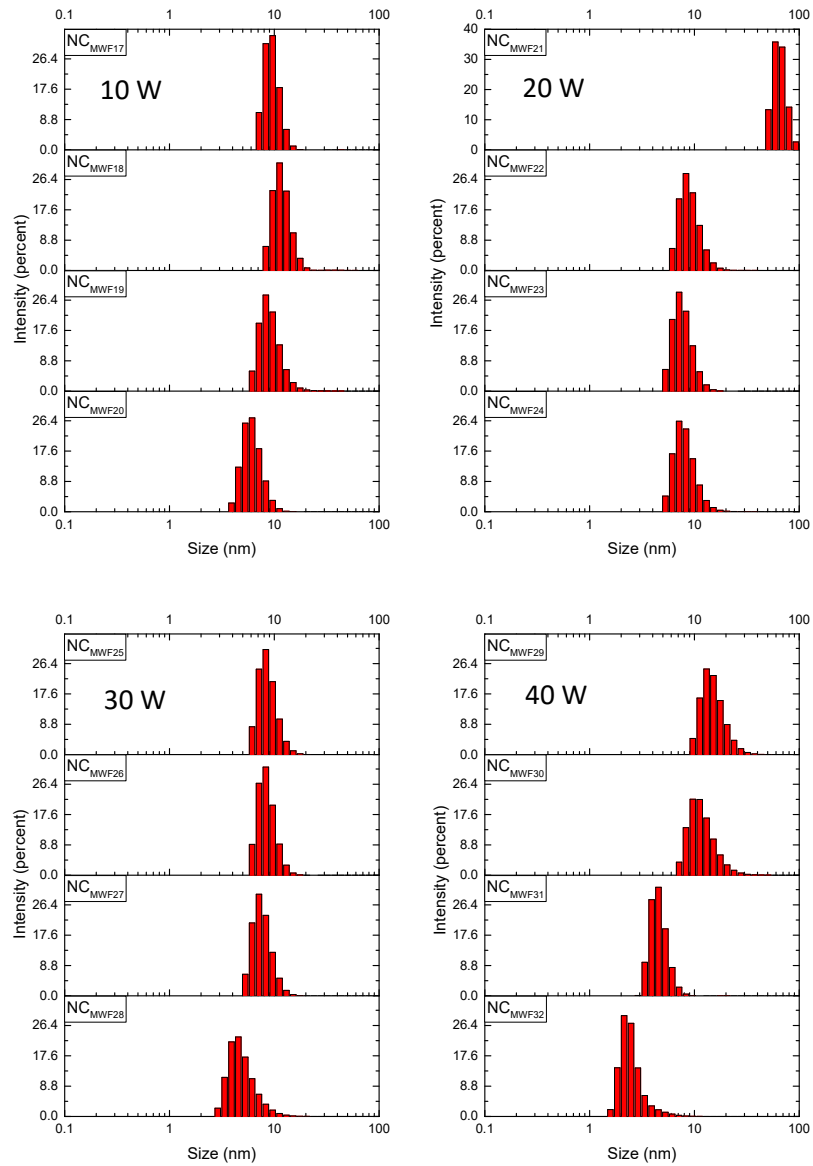


**Figure S9** Hydrodynamic size distribution of NC<sub>MWF17-32</sub>.

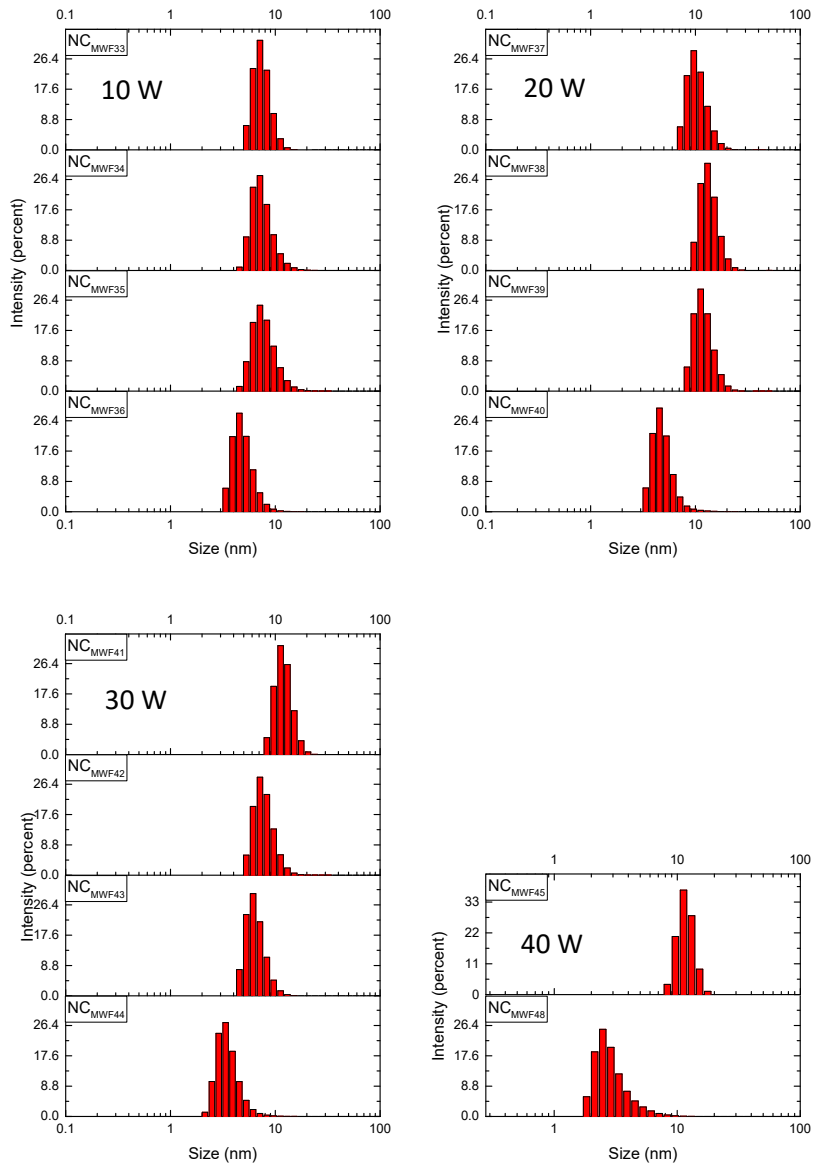


**Figure S10** Hydrodynamic size distribution of NC<sub>MWF33-45</sub> and NC<sub>MWF48</sub>.

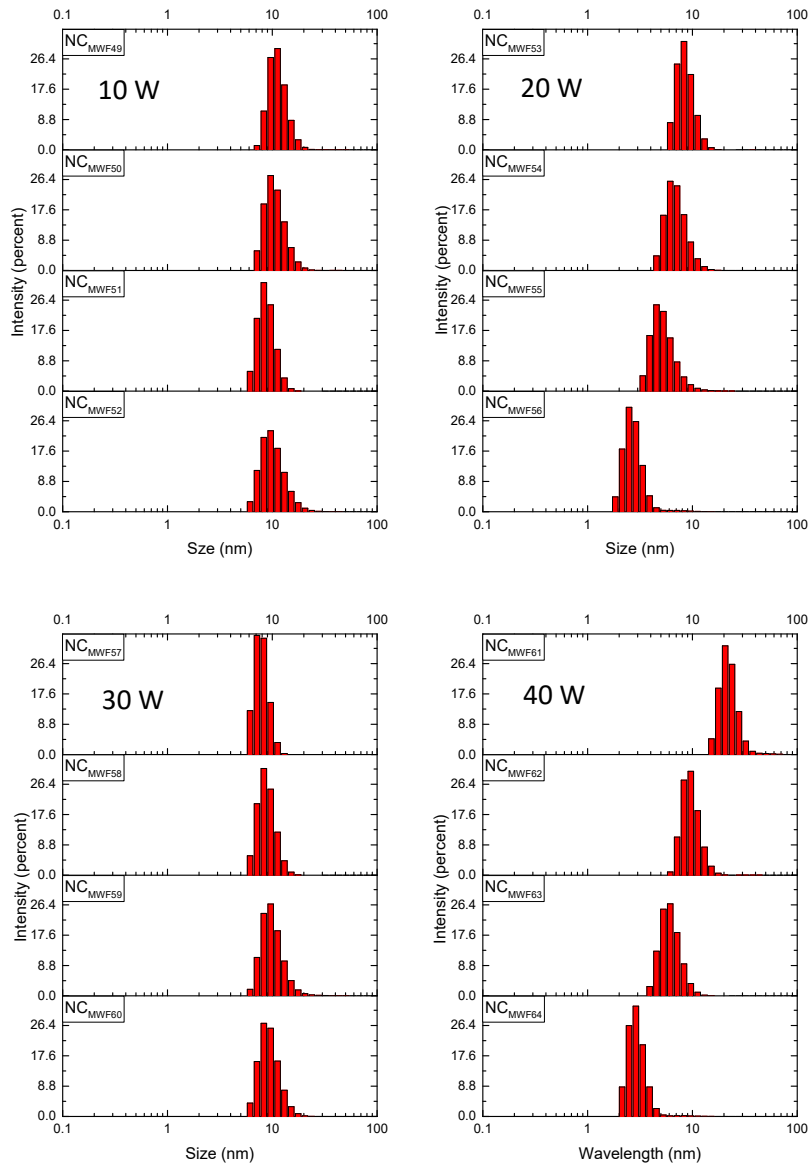


**Figure S11** Hydrodynamic size distribution of NC<sub>MWF49-64</sub>.

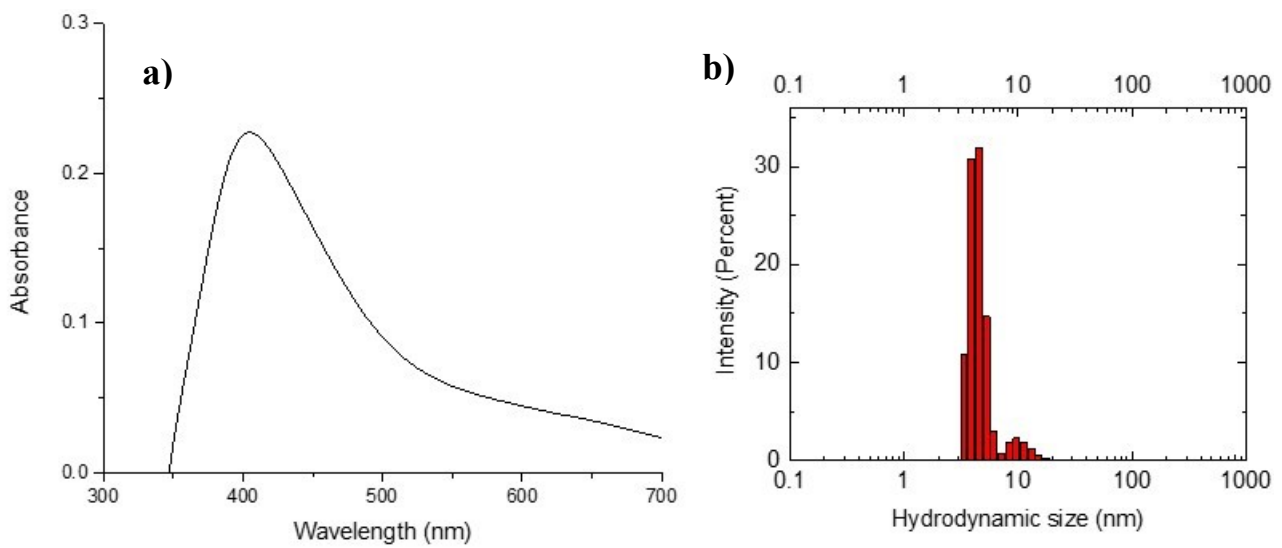


**Figure S12** a) UV-vis spectrum and b) hydrodynamic size distribution of AgNP/PA6 NC prepared using a 5-fold excess of PA6 under the same experimental conditions of NC<sub>MWF64</sub>.

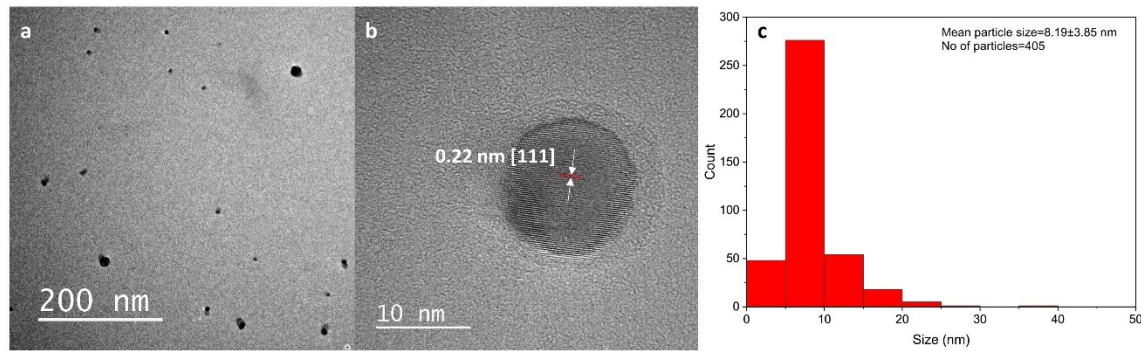


**Figure S13** a) TEM image of the prepared NC<sub>MWF32</sub>. b) HRTEM image of AgNPs embedded in the matrix of PA6. Red parallel lines exhibit the lattice fringe of AgNPs. The measured distance of 0.22 nm corresponds to [111] lattice plane c) The particle size distribution related to produced AgNPs.

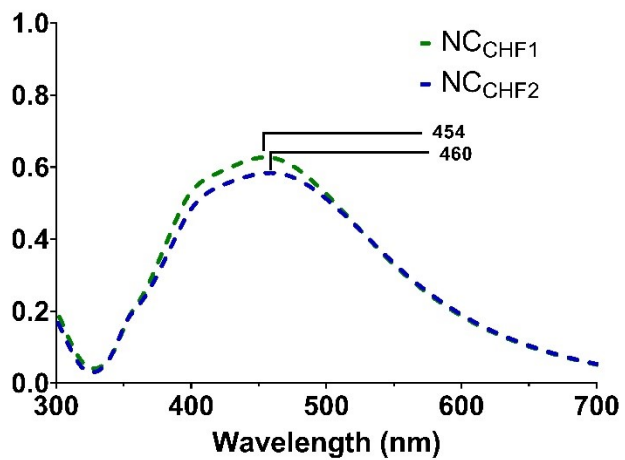


**Figure S14** UV-Vis spectra of the prepared NCs using the NaBH<sub>4</sub>:PA6/AgNO<sub>3</sub> FR ratios of 3:1 in the conventional heating fluidic system at 50 °C (NC<sub>CHF1</sub>) and 55 °C (NC<sub>CHF2</sub>).

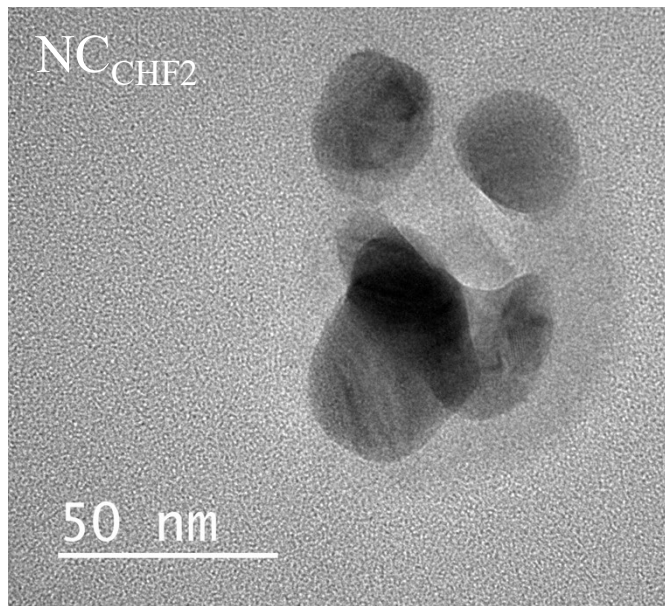


**Figure S15** TEM image of the AgNPs in NC<sub>CHF2</sub>.

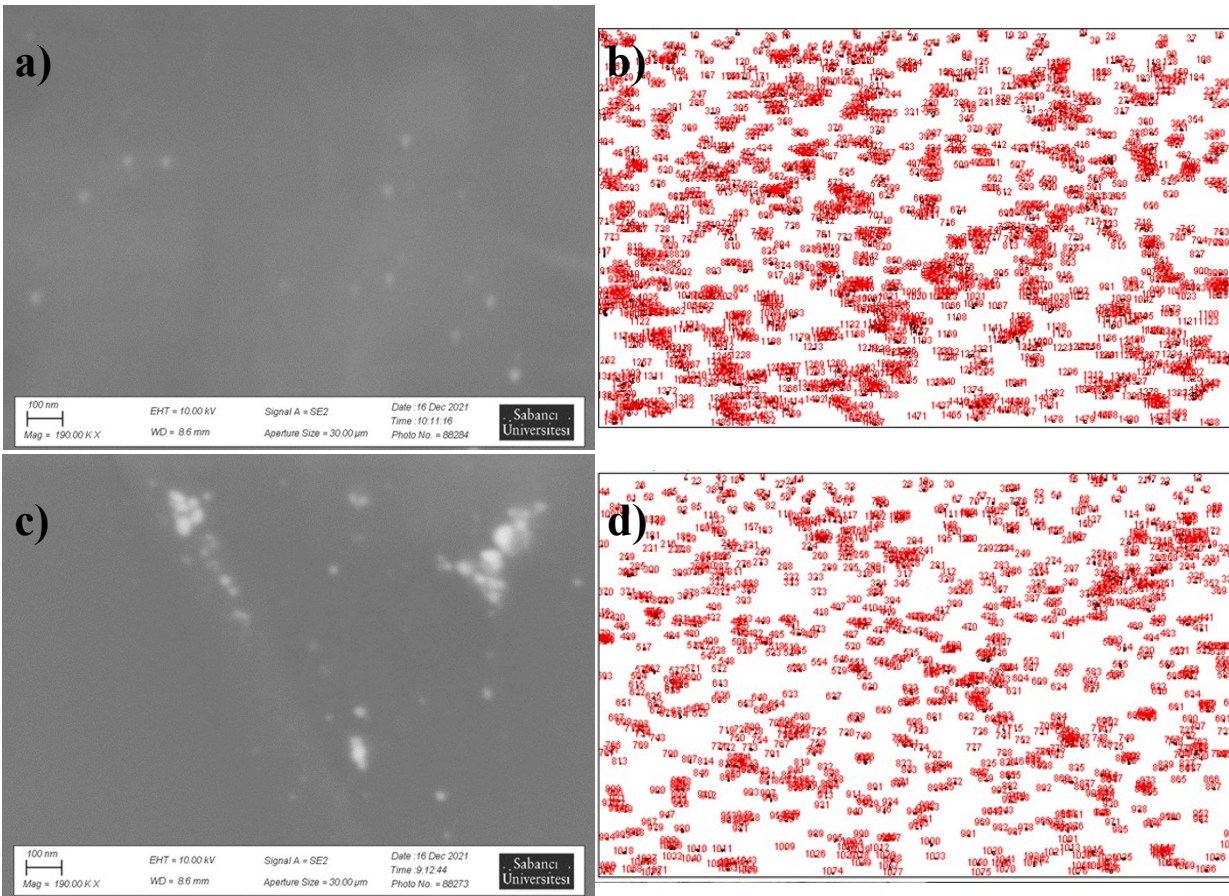
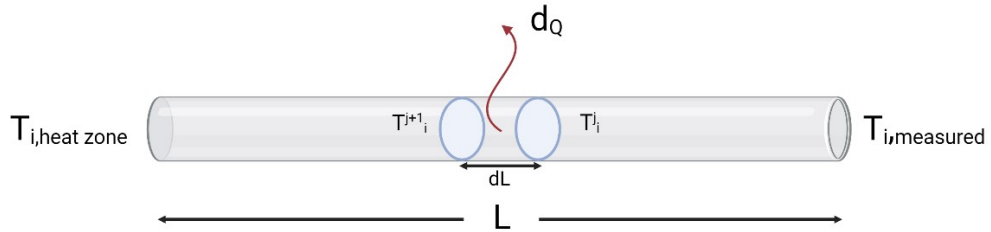


**Figure S16** SEM images (a and c) and EDX mapping analysis (b and d) of the prepared NC<sub>MWF64</sub> and NC<sub>CHF2</sub> films, respectively. The spot analysis was performed using ImageJ software. The threshold used was 6-255 for both images.

**Table S1** The estimated fluid temperatures outside the microwave heating zone.

Flow rate (FR) of NaBH <sub>4</sub> : FR of PA6/AgNO <sub>3</sub>	3:1					MWP=40 W		
	10	20	30	40	50	3:0.5	3:0.25	3:0.1
Measured temperature by using a thermocouple (°C)	36	38	40	50	110	47	53	53
Estimated exit temperature (°C)	39.87	41.87	43.87	53.87	113.87	50.87	56.87	56.87

The temperature of the fluid at the heating zone was estimated by measuring product temperature at 11cm away from this zone. For this measurement, the heat flow between fluid crossing through tubes of developed setup and air was considered convection.



Regarding the laminar flow in the piping system, the nusselt number, which depends on the inner diameter of the tubing system, fluid thermal conductivity, and convective heat transfer coefficient, is of great importance. For uniform heat transfer, the nusselt number is as follows,

$$\text{Nu}_D = 48/11 \cong 4.36$$

Considering the heat flow through the surface of tubes, the change in fluid temperature can be calculated in a small part of the tubes (dL) using the following formulas.

$$dQ = K_0 \pi d_0 (T_i^j - T_0) dL$$

$$K_0 = \left[ \frac{d_0}{h_i d_i} + \frac{d_0}{2\lambda f} \ln \frac{d_0}{d_i} + \frac{1}{h_0} \right]^{-1}$$

$$T_i^{j+1} = \frac{dQ}{mCp} + T_i^j$$

Due to the low content of AgNPs in fluid, formic acid characteristics were utilized for the following calculations. The calculated temperatures of fluid at 11cm away from the heating zone of MW for various MW powers and ratios of flow rate are provided in **Table S1**.

**Table S2** The calculated final concentrations of PA6, AgNO<sub>3</sub>, and NaBH<sub>4</sub> at varying FR ratios.

	PA6 (mg)	AgNO <sub>3</sub> (mol/L)	NaBH <sub>4</sub> (mol/L)	Total Volume@T-junction (mL)
	1	0.0005	0.002	
Flow rates (mL/min)		1	<b>3</b>	4
Final PA6 (mg/mL)	0.25			
Final AgNO <sub>3</sub> (mol/L)		0.000125		
Final NaBH <sub>4</sub> (mol/L)			0.0015	
	PA6 (mg)	AgNO <sub>3</sub> (mol/L)	NaBH <sub>4</sub> (mol/L)	Total Volume@T-junction (mL)
	1	0.0005	0.002	
Flow rates (mL/min)		0.5	<b>3</b>	3.5
Final PA6 (mg/mL)	0.142857143			
Final AgNO <sub>3</sub> (mol/L)		7.14286E-05		
Final NaBH <sub>4</sub> (mol/L)			0.001714286	
	PA6 (mg)	AgNO <sub>3</sub> (mol/L)	NaBH <sub>4</sub> (mol/L)	Total Volume@T-junction (mL)
	1	0.0005	0.002	
Flow rates (mL/min)		0.25	<b>3</b>	3.25
Final PA6 (mg/mL)	0.076923077			

Final AgNO <sub>3</sub> (mol/L)		3.84615E-05		
Final NaBH <sub>4</sub> (mol/L)			0.001846154	
	PA6 (mg)	AgNO <sub>3</sub> (mol/L)	NaBH <sub>4</sub> (mol/L)	Total Volume@T-junction (mL)
	1	0.0005	0.002	
Flow rates (mL/min)		0.1	<b>3</b>	3.1
Final PA6 (mg/mL)	0.032258065			
Final AgNO <sub>3</sub> (mol/L)		1.6129E-05		
Final NaBH <sub>4</sub> (mol/L)			0.001935484	
	PA6 (mg)	AgNO <sub>3</sub> (mol/L)	NaBH <sub>4</sub> (mol/L)	Total Volume@T-junction (mL)
	2	0.0005	0.002	
Flow rates (mL/min)		1	<b>3</b>	4
Final PA6 (mg/mL)	0.5			
Final AgNO <sub>3</sub> (mol/L)		0.000125		
Final NaBH <sub>4</sub> (mol/L)			0.0015	
	PA6 (mg)	AgNO <sub>3</sub> (mol/L)	NaBH <sub>4</sub> (mol/L)	Total Volume@T-junction (mL)
	2	0.0005	0.002	
Flow rates (mL/min)		0.5	<b>3</b>	3.5
Final PA6 (mg/mL)	0.285714286			
Final AgNO <sub>3</sub> (mol/L)		7.14286E-05		
Final NaBH <sub>4</sub> (mol/L)			0.001714286	

	PA6 (mg)	AgNO <sub>3</sub> (mol/L)	NaBH <sub>4</sub> (mol/L)	Total Volume@T-junction (mL)
	2	0.0005	0.002	
Flow rates (mL/min)		0.25	<b>3</b>	3.25
Final PA6 (mg/mL)	0.153846154			
Final AgNO <sub>3</sub> (mol/L)		3.84615E-05		
Final NaBH <sub>4</sub> (mol/L)			0.001846154	
	PA6 (mg)	AgNO <sub>3</sub> (mol/L)	NaBH <sub>4</sub> (mol/L)	Total Volume@T-junction (mL)
	2	0.0005	0.002	
Flow rates (mL/min)		0.1	<b>3</b>	3.1
Final PA6 (mg/mL)	0.064516129			
Final AgNO <sub>3</sub> (mol/L)		1.6129E-05		
Final NaBH <sub>4</sub> (mol/L)			0.001935484	
	PA (mg)	AgNO <sub>3</sub> (mol/L)	NaBH <sub>4</sub> (mol/L)	Total Volume@T-junction (mL)
	4	0.0005	0.002	
Flow rates (mL/min)		1	<b>3</b>	4
Final PA6 (mg/mL)	1			
Final AgNO <sub>3</sub> (mol/L)		0.000125		
Final NaBH <sub>4</sub> (mol/L)			0.0015	
	PA (mg)	AgNO <sub>3</sub> (mol/L)	NaBH <sub>4</sub> (mol/L)	Total Volume@T-junction (mL)
	4	0.0005	0.002	
Flow rates (mL/min)		0.5	<b>3</b>	3.5

Final PA6 (mg/mL)	0.571428571			
Final AgNO <sub>3</sub> (mol/L)		7.14286E-05		
Final NaBH <sub>4</sub> (mol/L)			0.001714286	
	PA (mg)	AgNO <sub>3</sub> (mol/L)	NaBH <sub>4</sub> (mol/L)	Total Volume@T-junction (mL)
	4	0.0005	0.002	
Flow rates (mL/min)		0.25	<b>3</b>	3.25
Final PA6 (mg/mL)	0.307692308			
Final AgNO <sub>3</sub> (mol/L)		3.84615E-05		
Final NaBH <sub>4</sub> (mol/L)			0.001846154	
	PA (mg)	AgNO <sub>3</sub> (mol/L)	NaBH <sub>4</sub> (mol/L)	Total Volume@T-junction (mL)
	4	0.0005	0.002	
Flow rates (mL/min)		0.1	<b>3</b>	3.1
Final PA6 (mg/mL)	0.129032258			
Final AgNO <sub>3</sub> (mol/L)		1.6129E-05		
Final NaBH <sub>4</sub> (mol/L)			0.001935484	
	PA (mg)	AgNO <sub>3</sub> (mol/L)	NaBH <sub>4</sub> (mol/L)	Total Volume@T-junction (mL)
	8	0.0005	0.002	
Flow rates (mL/min)		1	<b>3</b>	4
Final PA6 (mg/mL)	2			
Final AgNO <sub>3</sub> (mol/L)		0.000125		
Final NaBH <sub>4</sub> (mol/L)			0.0015	

	PA (mg)	AgNO <sub>3</sub> (mol/L)	NaBH <sub>4</sub> (mol/L)	Total Volume@T- junction (mL)
	8	0.0005	0.002	
Flow rates (mL/min)		0.5	<b>3</b>	3.5
Final PA6 (mg/mL)	1.142857143			
Final AgNO <sub>3</sub> (mol/L)		7.14286E-05		
Final NaBH <sub>4</sub> (mol/L)			0.001714286	
	PA (mg)	AgNO <sub>3</sub> (mol/L)	NaBH <sub>4</sub> (mol/L)	Total Volume@T- junction (mL)
	8	0.0005	0.002	
Flow rates (mL/min)		0.25	<b>3</b>	3.25
Final PA6 (mg/mL)	0.615384615			
Final AgNO <sub>3</sub> (mol/L)		3.84615E-05		
Final NaBH <sub>4</sub> (mol/L)			0.001846154	
	PA (mg)	AgNO <sub>3</sub> (mol/L)	NaBH <sub>4</sub> (mol/L)	Total Volume@T- junction (mL)
	8	0.0005	0.002	
Flow rates (mL/min)		0.1	<b>3</b>	3.1
Final PA6 (mg/mL)	0.258064516			
Final AgNO <sub>3</sub> (mol/L)		1.6129E-05		
Final NaBH <sub>4</sub> (mol/L)			0.001935484	